Title: Clinical and Genetic Features of Choroideraemia in Childhood.

Article Type: Manuscript

Corresponding Author: Mr. Kamron Khan,

Corresponding Author's Institution: leeds institute of molecular medicine

First Author: Kamron N Khan, PhD, FRCOphth

Order of Authors: Kamron N Khan, PhD, FRCOphth; Farrah Islam,
MBBS,FCPS,FRCS; Anthony Moore, FRCS, FRCOPhth; Michel Michaelides,
MD(Res) FRCOphth

Abstract: Clinical and Genetic Features of Choroideraemia in Childhood.

Kamron N Khan PhD, FRCOphth[1-3], Farrah Islam FCPS,FRCS[2], Anthony T
Moore FRCS, FRCOphth[1,2,4], Michel Michaelides MD(Res) FRCOphth[1,2]
1. University College London Institute of Ophthalmology, University
College London, London, UK.
2. Medical Retina Service, Moorfields Eye Hospital, London, UK.
3. Department of Ophthalmology, Leeds Institute of Molecular Medicine, St
James's University Hospital, Beckett St, Leeds, UK.
4. Ophthalmology Department, University of California San Francisco
Medical School, San Francisco, California, USA.

Abbreviations/Acronyms
Choroideraemia (CHM)
Rab escort protein-1 (REP-1)
Spectralis confocal scanning laser ophthalmoscope (cSLO)
Spectral Domain optical coherence tomography (SD-OCT)
Fundus autofluorescence (AF)
Internal limiting membrane (ILM)
Retinal pigment epithelium/Bruch membrane (RPE/BM)
Multiplex ligation dependent probe amplification (MLPA)
Choroidal neovascularisation (CNVM)
X-linked retinitis pigmentosa (XLRP)
Outer retinal tubulation (ORT)
Inner nuclear layer (INL)
Macular oedema (MO)
Late-onset retinal degeneration (L-ORD)
ATP-Binding Cassette, Subfamily A, Member 4 (ABCA4).

Clinical and Genetic Features of Choroideraemia in Childhood.
1. Objective or Purpose: To review the functional and anatomical
characteristics of choroideraemia in the paediatric population, aiming to
describing the earliest features of disease, and identify biomarkers
useful for monitoring disease progression.

2. Design: Retrospective, case series.
3. Subjects, Participants, and/or Controls: Children diagnosed with choroideraemia at a single institution.
4. Methods, Intervention, or Testing: Subjects were identified using an electronic patient record system. Case notes and retinal imaging (colour fundus photography (CFP), spectral domain optical coherence tomography (SD-OCT) and fundus autofluorescence (FAF)) were then reviewed. The results of genetic testing were also recorded.
5. Main Outcome Measures: Presenting symptoms, visual acuity, fundus changes (CFP, SD-OCT, FAF) and CHM sequencing results.
6. Results: 29 patients were identified with a mean age at referral of 9 years (range 3-16). CHM mutations were identified in 15/19 patients tested. Nyctalopia was the predominant symptom (66%). 5/29 patients were asymptomatic at presentation. At the final follow up visit (mean age 16, range 7-26) the majority maintained excellent visual acuity (mean 0.98 +/- 0.13 decimalized Snellen acuity). The first sign of retinopathy was widespread pigment clumping at the level of the retinal pigment epithelium (RPE). This later evolved to chorioretinal atrophy, most marked in the mid-peripheral retina. Peripapillary atrophy was also an early feature, and progressive in nature. Three different zones of FAF change were visible. Persistence of the inner retinal layers, detected by SD-OCT, was visible at presentation in 15/27 patients. Subfoveal choroidal thickness decreased with age whilst central retinal thickness increased over a similar interval. Four patients in whom visual acuity decreased over the follow-up period recorded a reduction in central retinal thickness.
7. Conclusions: Progressive structural changes occur at a time when central visual function is maintained. Pigmentary changes at the level of the RPE occur early in the disease course. Peripapillary chorioretinal atrophy, central retinal thickness and subfoveal choroidal thickness are likely to be valuable in monitoring disease progression, and should be considered as potential biomarkers in future therapeutic trials.

Point-by-point response to reviewers' comments.

Dear Editors,

Thank you very much for sending our manuscript for external review.

As recommended, please find below a point-by-point response to the comments provided.

Many thanks for considering this revised version for publication.

Kind Regards
Kamron

Mr Kamron Khan MB BChir MA PhD FRCOphth
Honorary Consultant Ophthalmologist
Moorfields Eye Hospital, London and St. James's Hospital, Leeds

Comment from Reviewer 1	Response	Changes made to text
Was foveal thickening due to the retained inner retinal layers or was the ONL also thickened?	Thank you. We have tried to address this in the text: "Persistence of the inner retinal layers was observed in 15/27 cases" (line 201). A further sentence confirming absence of ONL oedema has been added.	Text added for clarity, please see lines 203-204
Do the authors have visual field, microperimetry, or electrophysiology data? It would be a shame not to include these data if available.	Unfortunately these investigations are not routinely performed in an NHS clinic. Consequently these data are not available We agree that this information would be useful and add to our current knowledge of CHM and we aim to collect these data as part of a prospective natural history study.	
Comment from Reviewer 2	**Response**	**Changes made to text**
The authors should state the time period (years and months) for the patient visits that were part of this retrospective study.	Thank you. This information is included in the Table.	Changes made to the follow-up column in the Table. Time is recorded in years and decimalised months.
…it is recommended that the authors include wording to the effect that the chart review returned "Twenty-nine patients (28 pedigrees) were identified where the initial visit was under the age of 17 years."	Thank you. We agree.	Text has been added for clarity, please see lines 127-8.

Other reports have described patients with chroideremia in later stages of the disease where peripapillary sparing of the RPE/choriocapillaris was evident. Was this seen with any of the children as they got older? Was it observed in older affected family members of any of the pedigrees?	Thank you. We have reviewed the images of patients in this cohort, and where available their affected or carrier relatives. Peripapillary sparing was not observed, even in the most hyperopic individuals.	
The authors should consider referencing the recent report of occurrence of CNV with subretinal fibrosis presenting in a 13 year-old male with familial choroideremia. Palejwala NV, et al. Choroideremia associated with choroidal neovascularization treated with intravitreal bevacizumab. Clinical Ophthalmology 2014 8:1675-1679.	Thank you. We agree. This is similar to patient 10 in our series.	Text has been added for clarity, lines 341-5 and reference 18.
…the authors should consider making a table that emphasizes the earliest symptoms and findings of choroideremia and the youngest ages that they have observed these features.	Thank you. Findings of widespread pigmentary change, persistence of the inner retinal layers, and progressive sub-foveal choroidal thinning were visible as soon as retinal imaging was possible. One 5 year old displays all these features. In order to determine the exact order in which these occur we plan to prospectively	Please see lines 357-9. Rather than include a table stating "age 5" in all columns we have inserted a sentence noting that these signs were evident in the youngest patients in our cohort.

	investigate this.	

<u>Précis</u>

This work describes in detail the clinical features of choroideraemia in childhood. We present novel features of disease and propose biomarkers which will be useful in monitoring disease progression and response to future therapies.

1   **<u>Clinical and Genetic Features of Choroideraemia in Childhood.</u>**

2   Kamron N Khan PhD, FRCOphth[1-3], Farrah Islam FCPS,FRCS[2], Anthony T Moore

3   FRCS, FRCOphth[1,2,4], Michel Michaelides MD(Res) FRCOphth[1,2]

4   1. University College London Institute of Ophthalmology, University College London,

5   London, UK.

6   2. Medical Retina Service, Moorfields Eye Hospital, London, UK.

7   3. Department of Ophthalmology, Leeds Institute of Molecular Medicine, St James's

8   University Hospital, Beckett St, Leeds, UK.

9   4. Ophthalmology Department, University of California San Francisco Medical

10   School, San Francisco, California, USA.

13   Running Head: Khan et al/ Clinical & Genetic Features: Paediatric Choroideremia.

14   **Abbreviations/Acronyms**

15   Choroideraemia (CHM)

16   Rab escort protein-1 (REP-1)

17   Spectralis confocal scanning laser ophthalmoscope (cSLO)

18   Spectral Domain optical coherence tomography (SD-OCT)

19   Fundus autofluorescence (AF)

20   Internal limiting membrane (ILM)

21   Retinal pigment epithelium/Bruch membrane (RPE/BM)

22   Multiplex ligation dependent probe amplification (MLPA)

23   Choroidal neovascularisation (CNVM)

24   X-linked retinitis pigmentosa (XLRP)

25   Outer retinal tubulation (ORT)

26   Inner nuclear layer (INL)

27   Macular oedema (MO)

28   Late-onset retinal degeneration (L-ORD)

29   ATP-Binding Cassette, Subfamily A, Member 4 (ABCA4).

30

Clinical and Genetic Features of Choroideraemia in Childhood.

1. <u>Objective or Purpose</u>: To review the functional and anatomical characteristics of choroideraemia in the paediatric population, aiming to describing the earliest features of disease, and identify biomarkers useful for monitoring disease progression.

2. <u>Design</u>: Retrospective, case series.

3. <u>Subjects, Participants, and/or Controls</u>: Children diagnosed with choroideraemia at a single institution.

4. <u>Methods, Intervention, or Testing</u>: Subjects were identified using an electronic patient record system. Case notes and retinal imaging (colour fundus photography (CFP), spectral domain optical coherence tomography (SD-OCT) and fundus autofluorescence (FAF)) were then reviewed. The results of genetic testing were also recorded.

5. <u>Main Outcome Measures</u>: Presenting symptoms, visual acuity, fundus changes (CFP, SD-OCT, FAF) and *CHM* sequencing results.

6. <u>Results</u>: 29 patients were identified with a mean age at referral of 9 years (range 3-16). *CHM* mutations were identified in 15/19 patients tested. Nyctalopia was the predominant symptom (66%). 5/29 patients were asymptomatic at presentation. At the final follow up visit (mean age 16, range 7-26) the majority maintained excellent visual acuity (mean 0.98 +/- 0.13 decimalized Snellen acuity). The first sign of retinopathy was widespread pigment clumping at the level of the retinal pigment epithelium (RPE). This later evolved to chorioretinal

53 atrophy, most marked in the mid-peripheral retina. Peripapillary atrophy was also

54 an early feature, and progressive in nature. Three different zones of FAF change

55 were visible. Persistence of the inner retinal layers, detected by SD-OCT, was

56 visible at presentation in 15/27 patients. Subfoveal choroidal thickness decreased

57 with age whilst central retinal thickness increased over a similar interval. Four

58 patients in whom visual acuity decreased over the follow-up period recorded a

59 reduction in central retinal thickness.

60 7. Conclusions: Progressive structural changes occur at a time when central visual

61 function is maintained. Pigmentary changes at the level of the RPE occur early in

62 the disease course. Peripapillary chorioretinal atrophy, central retinal thickness

63 and subfoveal choroidal thickness are likely to be valuable in monitoring disease

64 progression, and should be considered as potential biomarkers in future

65 therapeutic trials.

66

67 **Clinical and Genetic Features of Choroideraemia in Childhood**

68

69 **Introduction**

70

71 Choroideraemia (CHM, OMIM 303100) is a rare, X-linked progressive retinal

72 dystrophy that is estimated to affect between 1 in 50,000 to 1 in 100,000

73 individuals. Typically male patients experience childhood-onset nyctalopia,

74 followed by loss of peripheral visual field in their teenage years. However, most

75 retain good central acuity into the fifth decade of life. Carrier females typically

76 display a phenotype consistent with random X chromosome inactivation,

77 manifesting as irregular pigmentary change in the fundus. Usually their

78 symptoms if any are much milder than affected males, however a minority may

79 be significantly affected, but usually with less severe disease than for male

80 relatives.[1]

81

82 Choroideraemia occurs due to dysfunction of the Rab escort protein-1 (REP-1), a

83 consequence of pathological genetic variation in the *CHM* gene.[2] Single point

84 mutations (coding, splice site, intronic) or small structural variants cause

85 isolated retinal disease, but occasionally contiguous gene deletion syndromes

86 occur where the CHM phenotype may be seen in conjunction with extraocular

87 disease.[1] Irrespective of the genotype, the overall effect is of loss of REP-1

88 function. REP-1 is one of two Rab escort proteins (REPs), cytosolic molecular

89 chaperones that facilitate Rab prenylation - the addition of geranylgeranyl

90 groups, which enable reversible anchoring of Rab proteins to the cell

91   membrane.[3]

92   The mechanism of retinal degeneration however is poorly understood, and there

93   is still uncertainty regarding which cell type(s) are primarily affected.[4] To

94   improve our understanding in this key area, and in view of on-going and

95   anticipated interventional trials of novel therapies, the present study reviews the

96   anatomical characteristics of CHM in the paediatric population, with the aim of

97   describing the earliest cellular patterns of degeneration.

98   **Methods**

99   A retrospective review of the electronic patient record system (OpenEyes,

100   Moorfields Eye Hospital (MEH), London, UK) was used to identify all children

101   (under the age of 17) diagnosed with choroideraemia. The patients' notes were

102   then reviewed along with the results of retinal imaging and molecular genetic

103   investigations.

104   Retinal imaging was performed using the Spectralis confocal scanning laser

105   ophthalmoscope (cSLO) (Heidelberg Engineering, Heidelberg, Germany) to

106   obtain spectral domain optical coherence tomography (SD-OCT) and 488nm

107   fundus autofluorescence (FAF) images. Subfoveal retinal and choroidal thickness

108   was assessed using the caliper function of the Heidelberg Eye Explorer software

109   (Heidelberg Engineering). The former was measured between the internal

110   limiting membrane (ILM) to the inner aspect of the retinal pigment

111   epithelium/Bruch membrane (RPE/BM) complex, whilst the latter was

112   measured from the outer aspect of the RPE/BM complex to anterior scleral

113   boundary. Retinal loci retaining physiological levels of autofluorescence were

114   measured using the "draw a region" function of the same software.

115   Genetic testing was performed by Sanger sequencing the entire coding sequence

116   of *CHM* at the national genetics reference laboratory (NGRL), Manchester, UK. If

117   no variants were identified, multiplex ligation dependent probe amplification

118   (MLPA) analysis was then performed in the same laboratory.

119   Statistical differences in paired data were analysed using a two-tailed paired

120   Student's T-test. For unpaired data a two sample, equal variance, two-tailed T-

121   test was performed.

122   This study was approved by the local research ethics committee, and all

123   investigations were conducted in accordance with the principles of the

124   Declaration of Helsinki.

125   **Results**

126   *Clinical Characteristics*

127   29 patients (28 pedigrees) were identified with a clinical diagnosis of CHM

128   where the initial visit was under the age of 17 years. Two patients were seen

129   only once, as they were referred for a second opinion regarding diagnosis. For all

130   other patients longitudinal data were available. The mean age at referral was 9

131   years (range 3-16) and at final follow up was 16 years (range 7-26). Patient

132   demographics are presented in Table 1.

133   Genetic testing was initiated in 19/29 cases and pathogenic variants were

134   identified in all but four cases (three pedigrees) (Table 1). Two of these three

135   families described a family history of eye disease, where affected male relatives

7

136 were more severely affected than females. In all three cases mothers displayed

137 the typical fundus features of a CHM carrier, despite the molecular cause

138 remaining elusive. In contrast, for one proband with molecularly confirmed

139 disease (patient 23) clinical examination of his mother was unremarkable, and

140 genetic testing confirmed the absence of her son's mutation. It is possible that

141 maternal germline mosaicism could account for this family's disease, although

142 this hypothesis was not tested further. In 10/29 cases (nine families) no testing

143 was performed; in all cases there was either an affected male relative (n=5) or

144 characteristic retinal changes present in the mother (n=5), consequently the

145 diagnosis was never in doubt.

146 The majority of patients were symptomatic at disease discovery, with 66%

147 (19/29) reporting difficulty seeing in the dark as their major concern, whilst in a

148 minority (17% or 5/29), the primary complaint was of peripheral field loss. A

149 similar number were asymptomatic (5/29), although this group did not differ

150 significantly in age from those who were symptomatic (mean age symptomatic =

151 9.6 years versus asymptomatic = 6.8 years, p = 0.15). In two cases the disease

152 was discovered on routine examination for assessment of refractive error. For

153 the majority of cases, central visual acuity at the initial visit was excellent (0.92

154 +/- 0.19 decimalized Snellen acuity). Correction of any refractive error resulted

155 in further improvement during the follow up period such that normal acuity was

156 maintained at the final clinic visit (mean acuity 0.98 +/- 0.13 decimalized Snellen

157 acuity).

158 *Retinal Imaging*

159 Colour fundus photography from at least one clinic visit was available for review

160   in 25/29 cases. The earliest identifiable changes were seen throughout the

161   peripheral retina, as pigmentary disturbance, thought to be external to the retina

162   and at the level of the RPE. The changes appeared as granular clumps of

163   pigmentation, finer at the macula than in the periphery (Figure 1a, b). Also

164   present at an early stage was peripapillary retinal atrophy (Figure 1c). With time

165   the areas of peripheral retina covered with pigmentary change evolved into

166   areas of atrophy, particularly well defined in the mid-peripheral retina, between

167   the vascular arcades and the equator (Fig 1c). Interspersed between these areas

168   of atrophy were regions that retained pigmentation, although ultimately these

169   were lost as the disease progressed. Later, regions of pigmented plaques were

170   visible. The peri and para-papillary atrophy was progressive, and advanced in a

171   centrifugal manner towards the macula (Figure 1d-g).

172   All four asymptomatic cases displayed significant retinal signs of disease. In

173   cases where the far periphery was imaged, the anterior retina appeared to have

174   more diffuse changes, with well circumscribed areas of atrophy being found

175   posterior to this (patients 10,15, 20, 21, 24, 26) (Figure h, i). In the most

176   advanced stages of disease, only the largest choroidal vessels were visible, with

177   complete loss of the choriocapillaris. The retinal vasculature however remained

178   subjectively unchanged, even when only a small central island of functioning

179   retina remained.

180   Fundus autofluorescence imaging was undertaken in 25/29 cases, with follow up

181   data available for 4/25. In all patients the area of normal FAF appeared to

182   correlate with age, although there was significant variation between individuals.

183   Eyes of the same patient however demonstrated significant symmetry (Student's

184 T-test, p=0.57). Where follow up data was available, all eyes demonstrated a

185 reduction in retained macular autofluorescence, with the most severely affected

186 eyes recording a slower rate of progression compared with those with milder

187 disease (patients 1 and 6 versus patients 5 and 7, Table 1). Loss of peri-papillary

188 autofluorescence was recorded early in the disease course, and this advanced as

189 the disease progressed (Figure 2a, b). In most cases, three patterns of FAF were

190 observed at the posterior pole: normal, speckled and absent (Figure 2c, d).

191 SD-OCT was used for both quantitative and qualitative analysis of retinal and

192 choroidal structure. Images were available for review in 27/29 cases, with

193 longitudinal data available for retinal and choroidal thickness in 17/27.

194 Significant fovea-involving macular oedema was not observed, consistent with

195 the excellent visual acuities recorded (Figure 3a, b). Localised intra-retinal

196 oedema was however seen at more peripheral loci, between zones of atrophic

197 and healthy tissue ("transition zones") where active degeneration would be

198 expected (Figure 3c). Outer retinal tubulation (ORT) was identified in similar

199 regions, in zones of recent atrophy adjacent to visibly normal tissue (Figure 3d).

200 Importantly ORT was never observed in regions of well-established atrophy,

201 suggesting residual photoreceptors and RPE are required (Figure 3d).

202 In 15/27 cases persistence of inner retinal layers (foveal hypoplasia) was visible

203 on macular line scans through the fovea (Figure 3a, b). Intraretinal oedema was

204 not evident in any of these cases. In 12/27 patients a normal foveal contour was

205 observed. On one scan (patient 10) posterior bowing of the line presumed to

206 represent Bruch membrane was observed in association with an irregular dome

207 shaped hyper-reflective mass (Figure 3e). This co-localised with a region of

208   subretinal fibrosis and was thought to relate to prior choroidal

209   neovascularisation (CNVM). Mild cystic spaces were identified in the inner

210   nuclear layer (INL) over regions where there was outer retinal architecture

211   distortion.

212   Subfoveal retinal and choroidal thickness measurements were recorded from

213   OCT scans. Central choroidal thickness decreased with increasing age, with a

214   mean thickness of $292 \pm 71\mu m$ early in the disease course (mean age 12), that

215   later reduced to $257 \pm 76\mu m$ (mean age 15, n=36 eyes) (p<0.00001). Over the

216   same time interval the subfoveal retinal thickness increased significantly, from

217    $232 \pm 46\mu m$ to $246 \pm 35\mu m$ (p=0.04) without visible retinal cysts. Whilst the

218   decrease in choroidal thickness was observed in all cases, a minority of eyes

219   showed a reduction in retinal thickness (n=8) rather than an increase (n=28).

220   Eyes in which a minor loss of acuity was noted (patients 23, 24, 27, 28) recorded

221   a mean reduction in retinal thickness (mean $7.6 \pm 13.2\mu m$) contrasting with eyes

222   where vision was maintained, which recorded a mean increase in retinal

223   thickness ($11.6 \pm 16.1\mu m$; p=0.017).

224

225   **Discussion**

226

227   This work provides a detailed retrospective analysis of the structural changes

228   seen in a large cohort of children with CHM. Until now, findings in this age group

229   have been scarce, and the few reported cases have been lost within a larger

230   volume of adult data. Consequently the earliest features of disease have been

231   poorly described.

232

233 Unlike most paediatric retinal dystrophies, which are discovered as a result of

234 reduced central acuity, CHM is most commonly identified as a result of

235 nyctalopia, and to a lesser degree loss of peripheral visual field. The youngest

236 patient to experience symptoms in this series was five years old, and so it is

237 likely that signs of retinopathy are present, yet undiscovered, at an early age.

238 With one exception, Patient 19, high refractive error was not a significant feature

239 of disease in keeping with other reports.[5] The low refractive error associated

240 with CHM also contrasts with the high myopia of X-linked retinitis pigmentosa

241 (XLRP), a potential phenocopy early in the disease course.

242

243 Maintenance of normal visual acuity is also in keeping with the absence of

244 significant macular oedema (MO), a feature reported to occur in up to 62.5% of

245 adult patients.[6] Early on in the disease course, a small increase in central retinal

246 thickness was noted in all patients with good central vision, perhaps indicating

247 subclinical microcystic oedema which was not easily visualised on OCT B scans.

248 Whilst the vast majority of eyes maintain baseline acuity, seven eyes recorded a

249 small deterioration in vision over the follow up period. The subfoveal retinal

250 thickness decreased in these eyes, acting perhaps as a surrogate marker of early

251 photoreceptor death. Over the same time period, almost all eyes showed a

252 reduction in subfoveal choroidal thickness. Despite the recognition of choroidal

253 atrophy in the first description of CHM, objective changes in choroidal thickness

254 have not previously been reported. Here we record a measurable reduction in

255 subfoveal choroidal thickness, detected at a time when central retinal function is

256 otherwise unaffected, and outside the zone of visible degeneration. This

257   discovery offers great clinical utility, as SD-OCT measurements of both retinal

258   and choroidal thickness, which have a low test-retest variability and can be

259   reliably obtained in virtually all subjects, will be useful both for monitoring

260   disease progression as well as response to novel therapies, independently of

261   visual acuity data.

262

263   Colour fundus photography was useful in identifying different stages of retinal

264   degeneration. Fourier et al. have previously used the same method to classify the

265   fundus changes present in female carriers of *CHM* mutations – mild RPE changes,

266   patchy RPE degeneration or confluent chorioretinal atrophy.[7] Identical

267   observations are reported here, but now in a paediatric cohort. Widespread

268   pigment clumping at the level of the RPE was identified as the earliest sign of

269   disease. This pigmentary response is very different to that observed in typical

270   retinitis pigmentosa, where RPE cells migrate into the neurosensory retina as a

271   consequence of photoreceptor cell death, usually resulting in a branched

272   network of "spicules". The pigment responsible for the observed changes has

273   two potential sources - melanosomes within the RPE, and melanocytes, thought

274   to be resident within the stroma of the choroid, both of which show significant

275   degeneration but for unknown reasons.[1] What *is* known is that REP-1

276   dysfunction, consequent upon *CHM* mutation, results in reduced Rab

277   prenylation.[8] Each Rab is uniquely sensitive to this process, based on its intrinsic

278   affinity for REP-1. Rab27a has a particularly low affinity when compared to other

279   Rabs, and as a result in a competitive environment, undergoes little prenylation.[8]

280   Rab27a dysfunction causes Griscelli syndrome (OMIM 607624), a disorder

281   characterized by hypomelanosis and immunological abnormalities. Rab27a is

282 now recognized not only as an important regulator of melanin transport in

283 melanosome, but also in polarized trafficking in (non-secretory) epithelial cells.[8]

284 It is therefore plausible that the observed retinal pigment clumping represents a

285 visible manifestation of local Rab27a-associated melanosome transport

286 dysfunction, and that other vesicle trafficking problems co-exist. Ultimately these

287 result in RPE disease and death. Unlike choroidal melanocytes, the RPE

288 melanosomes are fully mature at birth, and are incapable of renewal, perhaps

289 explaining why the RPE is so sensitive to REP-1 dysfunction.[9]

290

291 Following widespread pigmentary changes, well-defined regions of atrophy

292 develop, most commonly in the post-equatorial region, just outside the vascular

293 arcades. These changes advance centripetally whilst the far periphery seems to

294 be relatively spared. It is possible that this stereotypical feature of disease may

295 either relate to the underlying arrangement of lobular choroidal anatomy,

296 regional differences in RPE metabolism or indeed both, and explain why these

297 changes are not so readily seen in the anterior retina. A similar pattern of retinal

298 degeneration occurs in gyrate atrophy (OMIM 258870) and dominant mutation

299 of RPE65, but may also be observed in late-onset retinal degeneration (L-ORD,

300 OMIM 605670), all conditions that are thought to affect the RPE.[10]

301

302 Peri-papillary disease has been poorly described to date. In this series all

303 patients, even the youngest showed significant para- and peri-papillary atrophy.

304 Whilst objective analysis of the retinal nerve fibre layer in this region has been

305 performed, detailed assessment of the surrounding outer retina changes has not

306 been reported.[11-13] It is unclear why patients with CHM have early peri-papillary

14

307   involvement, whilst in retinal disease associated with biallelic *ABCA4* mutations

308   this retinal region is spared. One possibility is that choroidal blood flow may

309   influence the rate of progression, as degeneration in CHM appears to

310   preferentially occur in loci where the choroid is at its thinnest.

311

312   In addition to causing a progressive retinopathy, mutation of *CHM* could

313   theoretically also result in anatomical changes present at birth or shortly

314   thereafter. In keeping with this hypothesis, persistence of the inner retinal layers

315   was identified in approximately half of the cases (15/27), a similar finding to

316   that seen in patients with another disorder of hypomelanosis – albinism, where

317   variable degrees of foveal hypoplasia are observed.[14] In some cases however,

318   very dense scans through fixation were not obtained, so it remains possible that

319   a normal foveola exists but was just not captured. Usually however, the foveal pit

320   is large enough to be identifiable on at least two normal density macula line

321   scans, as such we feel that its absence is not due to technical factors. Again, in

322   keeping with incomplete foveal maturation, changes in central foveal

323   autofluorescence were also noted, perhaps indicating subtle alterations in the

324   amount of luteal pigment within Henle layer, a finding otherwise unexpected in

325   the earliest stages of many other retinal dystrophies. Lastly, macular hole

326   formation is an extremely uncommon complication of inherited retinal disease,

327   with only scattered single cases identified.[15] Unusually, a recent report describes

328   the prevalence of macular hole formation in patients with CHM at 10%, again

329   hinting at a possible underlying developmental macular anomaly.[16] Alternatively

330   this may either relate to a high prevalence of pre-retinal glial cell proliferation in

331   advanced disease resulting in mechanical traction from epiretinal membrane

332   tissue or the consequence of chronic cystic change.

333

334   Another feature associated with chorioretinal atrophy is ORT.[17] In our study ORT

335   was notably absent from regions of established atrophy, and only found adjacent

336   to healthy tissue, suggesting that the remaining (overhanging) photoreceptors

337   may organise themselves around residual islands of RPE cells. Other signs of

338   advanced atrophy, such as "ghost drusen" (highly reflective pyramidal

339   structures), a common feature of advanced L-ORD (unpublished observation),

340   are absent. Similarly, although late-stage retinal disease may also be complicated

341   by choroidal neovascularization (CNVM), this is thought to be an uncommon

342   feature of end-stage CHM. Cases of presumed CNVM, similar to that observed in

343   patient 10 do exist, and have been reported by others.[18] The true prevalence of

344   CNVM will be hard to determine however, as generally only symptomatic

345   patients are identified.

346

347

348   This study provides a detailed description of the clinical, imaging and genetic

349   findings present in a large cohort of paediatric patients with CHM. We propose

350   that the observed widespread pigmentary changes are a visible consequence of

351   Rab27a dysfunction, and highlight novel anatomical changes present both in the

352   peri-papillary retina and inner retina at the fovea. In addition, we have presented

353   SD-OCT data demonstrating a reduction in subfoveal choroidal thickness with

354   disease progression, and a simultaneous increase in foveal retinal thickness, both

355   of which occur whilst visual acuity is maintained. Deterioration in visual acuity is

356   uncommon in CHM in childhood but when it does occur it is associated with a

reduction in retinal thickness. <u>The anatomical changes described herein were evident even in the youngest patients, and hence must occur early in the disease course.</u> We envisage that these objective imaging parameters will become useful tools for monitoring change, both in prospective natural history studies of CHM and in response to future treatments.

<u>RFERENCES</u>

1.   Coussa RG, Traboulsi EI. Choroideremia: A review of general findings and pathogenesis. Ophthalmic Genetics 2012;33(2):57-65.

2.   Cremers F, 6Uniuersitéitszugenklinik EKU. Molecular Basis of Choroideremia (CHM): Mutations involving the Rab Escort Proteinal (REP-1) Gene. Human mutation 1997;9:110-7.

3.   Leung KF, Baron R, Seabra MC. Thematic review series: lipid posttranslational modifications. geranylgeranylation of Rab GTPases. J Lipid Res 2006;47(3):467-75.

4.   Pereira-Leal JB, Hume AN, Seabra MC. Prenylation of Rab GTPases: molecular mechanisms and involvement in genetic disease. FEBS letters 2001;498(2):197-200.

5.   Seitz IP, Zhour A, Kohl S, et al. Multimodal assessment of choroideremia patients defines pre-treatment characteristics. Graefe's Archive for Clinical and Experimental Ophthalmology 2015:1-8.

6.   Genead MA, Fishman GA. Cystic macular oedema on spectral-domain optical coherence tomography in choroideremia patients without cystic changes on fundus examination. Eye 2011;25(1):84-90.

381 7.   Forius H, Hyvainen L, Nieminen H, Flower R. FLuorescein and

382 Indocyanine green Fluorescence angiography in study of affected males and in

383 female carriers with Choroidermia. Acta ophthalmologica 1977;55(3):459-70.

384 8.   Köhnke M, Delon C, Hastie ML, et al. Rab GTPase prenylation hierarchy

385 and its potential role in choroideremia disease. PloS one 2013;8(12):e81758.

386 9.   Nag TC. Ultrastructural changes in the melanocytes of aging human

387 choroid. Micron 2015;79:16-23.

388 10.   Bowne SJ, Humphries MM, Sullivan LS, et al. A dominant mutation in

389 RPE65 identified by whole-exome sequencing causes retinitis pigmentosa with

390 choroidal involvement. Eur J Hum Genet 2011;19(10):1074-81.

391 11.   Genead MA, McAnany JJ, Fishman GA. Retinal nerve fiber thickness

392 measurements in choroideremia patients with spectral-domain optical

393 coherence tomography. Ophthalmic genetics 2011;32(2):101-6.

394 12.   Jiang R, Wang YX, Wei WB, et al. Peripapillary Choroidal Thickness in

395 Adult Chinese: The Beijing Eye StudyPeripapillary Choroidal Thickness.

396 Investigative ophthalmology & visual science 2015;56(6):4045-52.

397 13.   Read SA, Alonso-Caneiro D, Vincent SJ, Collins MJ. Peripapillary choroidal

398 thickness in childhood. Experimental eye research 2015;135:164-73.

399 14.   Lee H, Purohit R, Sheth V, et al. Retinal development in albinism: a

400 prospective study using optical coherence tomography in infants and young

401 children. The Lancet 2015;385:S14.

402 15.   Sodi A, Bini A, Passerini I, et al. Occurrence of full-thickness macular hole

403 complicating Stargardt disease with ABCR mutation. Eur J Ophthalmol

404 2006;16(2):335-8.

405   16.   Zinkernagel MS, Groppe M, MacLaren RE. Macular hole surgery in patients

406   with end-stage choroideremia. Ophthalmology 2013;120(8):1592-6.

407   17.   Iriyama A, Aihara Y, Yanagi Y. Outer retinal tubulation in inherited retinal

408   degenerative disease. Retina 2013;33(7):1462-5.

409   18.   Palejwala NV, Lauer AK and Weleber RG. Choroideremia associated with

410   choroidal neovascularization treated with intravitreal bevacizumab. Clinical

411   Ophthalmology 2014 8:1675-1679.

412

413

LEGENDS

Figure 1: Colour fundus photography in patients with choroideraemia. (a) Early,

fine, granular pigmentary changes in the central macula and around the vascular

arcades, (b) larger pigment plaques in the temporal periphery. (c) Four years

later the regions of pigmentary change have now evolved to atrophy, also

involving the peripapillary retina (patient 4). Images (d, e) and (f, g) taken from

patient 5 two years apart, highlighting progressive PPA. (h, i) Optos

pseudocolour images from patient 7 highlighting well defined scalloped atrophy

and pigment plaques with less well-defined anterior changes.

Figure 2: Fundus autofluorescence images demonstrating the progression in

peripapillary atrophy in patient 2 (a, b). Three distinct zones of autofluorescence

are visible in patient 6 – complete absence, speckled and normal (c, d).

Figure 3: Spectral domain optical coherence tomography in patients with

choroideraemia. Approximately half of all eyes demonstrated persistence of the

inner retinal layers (a, b). In regions immediately adjacent to atrophic retina, loss

of retinal structure was associated with the presence of cystic spaces in either

the outer or inner nuclear layers (c). Outer retinal tubulations were observed

only in regions retaining small islands of retinal pigment epithelium, but never in

areas of frank atrophy (d). Imaging the left eye of Patient 10 shows the presence

of highly reflective subretinal material, suggestive of prior choroidal

neovascularization (e).

1   <u>**Clinical and Genetic Features of Choroideraemia in Childhood.**</u>

2   Kamron N Khan PhD, FRCOphth[1-3], Farrah Islam FCPS,FRCS[2], Anthony T Moore

3   FRCS, FRCOphth[1,2,4], Michel Michaelides MD(Res) FRCOphth[1,2]

4   1. University College London Institute of Ophthalmology, University College London,

5   London, UK.

6   2. Medical Retina Service, Moorfields Eye Hospital, London, UK.

7   3. Department of Ophthalmology, Leeds Institute of Molecular Medicine, St James's

8   University Hospital, Beckett St, Leeds, UK.

9   4. Ophthalmology Department, University of California San Francisco Medical

10   School, San Francisco, California, USA.

14   **Abbreviations/Acronyms**

15   Choroideraemia (CHM)

16   Rab escort protein-1 (REP-1)

17   Spectralis confocal scanning laser ophthalmoscope (cSLO)

18   Spectral Domain optical coherence tomography (SD-OCT)

19   Fundus autofluorescence (AF)

20   Internal limiting membrane (ILM)

21   Retinal pigment epithelium/Bruch membrane (RPE/BM)

22   Multiplex ligation dependent probe amplification (MLPA)

23   Choroidal neovascularisation (CNVM)

24   X-linked retinitis pigmentosa (XLRP)

25   Outer retinal tubulation (ORT)

26   Inner nuclear layer (INL)   2

27   Macular oedema (MO)

28   Late-onset retinal degeneration (L-ORD)

29   ATP-Binding Cassette, Subfamily A, Member 4 (ABCA4).

30

31   **Clinical and Genetic Features of Choroideraemia in Childhood.**

32   1. <u>Objective or Purpose</u>: To review the functional and anatomical characteristics of

33   choroideraemia in the paediatric population, aiming to describing the earliest

34   features of disease, and identify biomarkers useful for monitoring disease

35   progression.

36   2. <u>Design</u>: Retrospective, case series.

37   3. <u>Subjects, Participants, and/or Controls</u>: Children diagnosed with

38   choroideraemia at a single institution.

39   4. <u>Methods, Intervention, or Testing</u>: Subjects were identified using an electronic

40   patient record system. Case notes and retinal imaging (colour fundus photography

41   (CFP), spectral domain optical coherence tomography (SD-OCT) and fundus

42   autofluorescence (FAF)) were then reviewed. The results of genetic testing were

43   also recorded.

44   5. <u>Main Outcome Measures</u>: Presenting symptoms, visual acuity, fundus changes

45   (CFP, SD-OCT, FAF) and *CHM* sequencing results.

46   6. <u>Results</u>: 29 patients were identified with a mean age at referral of 9 years (range

47   3-16). *CHM* mutations were identified in 15/19 patients tested. Nyctalopia was

48   the predominant symptom (66%). 5/29 patients were asymptomatic at

49   presentation. At the final follow up visit (mean age 16, range 7-26) the majority

50   maintained excellent visual acuity (mean 0.98 +/- 0.13 decimalized Snellen

51   acuity). The first sign of retinopathy was widespread pigment clumping at the

52   level of the retinal pigment epithelium (RPE). This later evolved to chorioretinal

53 atrophy, most marked in the mid-peripheral retina. Peripapillary atrophy was also

54 an early feature, and progressive in nature. Three different zones of FAF change

55 were visible. Persistence of the inner retinal layers, detected by SD-OCT, was

56 visible at presentation in 15/27 patients. Subfoveal choroidal thickness decreased

57 with age whilst central retinal thickness increased over a similar interval. Four

58 patients in whom visual acuity decreased over the follow-up period recorded a

59 reduction in central retinal thickness.

60 7. <u>Conclusions</u>: Progressive structural changes occur at a time when central visual

61 function is maintained. Pigmentary changes at the level of the RPE occur early in

62 the disease course. Peripapillary chorioretinal atrophy, central retinal thickness

63 and subfoveal choroidal thickness are likely to be valuable in monitoring disease

64 progression, and should be considered as potential biomarkers in future

65 therapeutic trials.

66

67   **Clinical and Genetic Features of Choroideraemia in Childhood**

68

69   **Introduction**

70

71   Choroideraemia (CHM, OMIM 303100) is a rare, X-linked progressive retinal

72   dystrophy that is estimated to affect between 1 in 50,000 to 1 in 100,000

73   individuals. Typically male patients experience childhood-onset nyctalopia,

74   followed by loss of peripheral visual field in their teenage years. However, most

75   retain good central acuity into the fifth decade of life. Carrier females typically

76   display a phenotype consistent with random X chromosome inactivation,

77   manifesting as irregular pigmentary change in the fundus. Usually their

78   symptoms if any are much milder than affected males, however a minority may

79   be significantly affected, but usually with less severe disease than for male

80   relatives.[1]

81

82   Choroideraemia occurs due to dysfunction of the Rab escort protein-1 (REP-1), a

83   consequence of pathological genetic variation in the *CHM* gene.[2] Single point

84   mutations (coding, splice site, intronic) or small structural variants cause

85   isolated retinal disease, but occasionally contiguous gene deletion syndromes

86   occur where the CHM phenotype may be seen in conjunction with extraocular

87   disease.[1] Irrespective of the genotype, the overall effect is of loss of REP-1

88   function. REP-1 is one of two Rab escort proteins (REPs), cytosolic molecular

89   chaperones that facilitate Rab prenylation - the addition of geranylgeranyl

90   groups, which enable reversible anchoring of Rab proteins to the cell

91   membrane.[3]

92   The mechanism of retinal degeneration however is poorly understood, and there

93   is still uncertainty regarding which cell type(s) are primarily affected.[4] To

94   improve our understanding in this key area, and in view of on-going and

95   anticipated interventional trials of novel therapies, the present study reviews the

96   anatomical characteristics of CHM in the paediatric population, with the aim of

97   describing the earliest cellular patterns of degeneration.

98   **Methods**

99   A retrospective review of the electronic patient record system (OpenEyes,

100   Moorfields Eye Hospital (MEH), London, UK) was used to identify all children

101   (under the age of 17) diagnosed with cho123eraemia. The patients' notes were

102   then reviewed along with the results of retinal imaging and molecular genetic

103   investigations.

104   Retinal imaging was performed using the Spectralis confocal scanning laser

105   ophthalmoscope (cSLO) (Heidelberg Engineering, Heidelberg, Germany) to

106   obtain spectral domain optical coherence tomography (SD-OCT) and 488nm

107   fundus autofluorescence (FAF) images. Subfoveal retinal and choroidal thickness

108   was assessed using the caliper function of the Heidelberg Eye Explorer software

109   (Heidelberg Engineering). The former was measured between the internal

110   limiting membrane (ILM) to the inner aspect of the retinal pigment

111   epithelium/Bruch membrane (RPE/BM) complex, whilst the latter was

112   measured from the outer aspect of the RPE/BM complex to anterior scleral

113   boundary. Retinal loci retaining physiological levels of autofluorescence were

114   measured using the "draw a region" function of the same software.

115   Genetic testing was performed by Sanger sequencing the entire coding sequence

116   of *CHM* at the national genetics reference laboratory (NGRL), Manchester, UK. If

117   no variants were identified, multiplex ligation dependent probe amplification

118   (MLPA) analysis was then performed in the same laboratory.

119   Statistical differences in paired data were analysed using a two-tailed paired

120   Student's T-test. For unpaired data a two sample, equal variance, two-tailed T-

121   test was performed.

122   This study was approved by the local research ethics committee, and all

123   investigations were conducted in accordance with the principles of the

124   Declaration of Helsinki.

125   **Results**

126   *Clinical Characteristics*

127   29 patients (28 pedigrees) were identified with a clinical diagnosis of CHM

128   where the initial visit was under the age of 17 years. Two patients were seen

129   only once, as they were referred for a second opinion regarding diagnosis. For all

130   other patients longitudinal data were available. The mean age at referral was 9

131   years (range 3-16) and at final follow up was 16 years (range 7-26). Patient

132   demographics are presented in Table 1.

133   Genetic testing was initiated in 19/29 cases and pathogenic variants were

134   identified in all but four cases (three pedigrees) (Table 1). Two of these three

135   families described a family history of eye disease, where affected male relatives

136   were more severely affected than females. In all three cases mothers displayed

137   the typical fundus features of a CHM carrier, despite the molecular cause

138   remaining elusive. In contrast, for one proband with molecularly confirmed

139   disease (patient 23) clinical examination of his mother was unremarkable, and

140   genetic testing confirmed the absence of her son's mutation. It is possible that

141   maternal germline mosaicism could account for this family's disease, although

142   this hypothesis was not tested further. In 10/29 cases (nine families) no testing

143   was performed; in all cases there was either an affected male relative (n=5) or

144   characteristic retinal changes present in the mother (n=5), consequently the

145   diagnosis was never in doubt.

146   The majority of patients were symptomatic at disease discovery, with 66%

147   (19/29) reporting difficulty seeing in the dark as their major concern, whilst in a

148   minority (17% or 5/29), the primary complaint was of peripheral field loss. A

149   similar number were asymptomatic (5/29), although this group did not differ

150   significantly in age from those who were symptomatic (mean age symptomatic =

151   9.6 years versus asymptomatic = 6.8 years, p = 0.15). In two cases the disease

152   was discovered on routine examination for assessment of refractive error. For

153   the majority of cases, central visual acuity at the initial visit was excellent (0.92

154   +/- 0.19 decimalized Snellen acuity). Correction of any refractive error resulted

155   in further improvement during the follow up period such that normal acuity was

156   maintained at the final clinic visit (mean acuity 0.98 +/- 0.13 decimalized Snellen

157   acuity).

158   *Retinal Imaging*

159   Colour fundus photography from at least one clinic visit was available for review

160   in 25/29 cases. The earliest identifiable changes were seen throughout the

161   peripheral retina, as pigmentary disturbance, thought to be external to the retina

162   and at the level of the RPE. The changes appeared as granular clumps of

163   pigmentation, finer at the macula than in the periphery (Figure 1a, b). Also

164   present at an early stage was peripapillary retinal atrophy (Figure 1c). With time

165   the areas of peripheral retina covered with pigmentary change evolved into

166   areas of atrophy, particularly well defined in the mid-peripheral retina, between

167   the vascular arcades and the equator (Fig 1c). Interspersed between these areas

168   of atrophy were regions that retained pigmentation, although ultimately these

169   were lost as the disease progressed. Later, regions of pigmented plaques were

170   visible. The peri and para-papillary atrophy was progressive, and advanced in a

171   centrifugal manner towards the macula (Figure 1d-g).

172   All four asymptomatic cases displayed significant retinal signs of disease. In

173   cases where the far periphery was imaged, the anterior retina appeared to have

174   more diffuse changes, with well circumscribed areas of atrophy being found

175   posterior to this (patients 10,15, 20, 21, 24, 26) (Figure h, i). In the most

176   advanced stages of disease, only the largest choroidal vessels were visible, with

177   complete loss of the choriocapillaris. The retinal vasculature however remained

178   subjectively unchanged, even when only a small central island of functioning

179   retina remained.

180   Fundus autofluorescence imaging was undertaken in 25/29 cases, with follow up

181   data available for 4/25. In all patients the area of normal FAF appeared to

182   correlate with age, although there was significant variation between individuals.

183   Eyes of the same patient however demonstrated significant symmetry (Student's

184   T-test, p=0.57). Where follow up data was available, all eyes demonstrated a

185   reduction in retained macular autofluorescence, with the most severely affected

186   eyes recording a slower rate of progression compared with those with milder

187   disease (patients 1 and 6 versus patients 5 and 7, Table 1). Loss of peri-papillary

188   autofluorescence was recorded early in the disease course, and this advanced as

189   the disease progressed (Figure 2a, b). In most cases, three patterns of FAF were

190   observed at the posterior pole: normal, speckled and absent (Figure 2c, d).

191   SD-OCT was used for both quantitative and qualitative analysis of retinal and

192   choroidal structure. Images were available for review in 27/29 cases, with

193   longitudinal data available for retinal and choroidal thickness in 17/27.

194   Significant fovea-involving macular oedema was not observed, consistent with

195   the excellent visual acuities recorded (Figure 3a, b). Localised intra-retinal

196   oedema was however seen at more peripheral loci, between zones of atrophic

197   and healthy tissue ("transition zones") where active degeneration would be

198   expected (Figure 3c). Outer retinal tubulation (ORT) was identified in similar

199   regions, in zones of recent atrophy adjacent to visibly normal tissue (Figure 3d).

200   Importantly ORT was never observed in regions of well-established atrophy,

201   suggesting residual photoreceptors and RPE are required (Figure 3d).

202   In 15/27 cases persistence of inner retinal layers (foveal hypoplasia) was visible

203   on macular line scans through the fovea (Figure 3a, b). Intraretinal oedema was

204   not evident in any of these cases. In 12/27 patients a normal foveal contour was

205   observed. On one scan (patient 10) posterior bowing of the line presumed to

206   represent Bruch membrane was observed in association with an irregular dome

207   shaped hyper-reflective mass (Figure 3e). This co-localised with a region of

208   subretinal fibrosis and was thought to relate to prior choroidal

209   neovascularisation (CNVM). Mild cystic spaces were identified in the inner

210   nuclear layer (INL) over regions where there was outer retinal architecture

211   distortion.

212   Subfoveal retinal and choroidal thickness measurements were recorded from

213   OCT scans. Central choroidal thickness decreased with increasing age, with a

214   mean thickness of 292 ± 71μm early in the disease course (mean age 12), that

215   later reduced to 257 ± 76μm (mean age 15, n=36 eyes) (p<0.00001). Over the

216   same time interval the subfoveal retinal thickness increased significantly, from

217   232 ± 46μm to 246 ± 35μm (p=0.04) without visible retinal cysts. Whilst the

218   decrease in choroidal thickness was observed in all cases, a minority of eyes

219   showed a reduction in retinal thickness (n=8) rather than an increase (n=28).

220   Eyes in which a minor loss of acuity was noted (patients 23, 24, 27, 28) recorded

221   a mean reduction in retinal thickness (mean 7.6 ± 13.2μm) contrasting with eyes

222   where vision was maintained, which recorded a mean increase in retinal

223   thickness (11.6 ± 16.1μm; p=0.017).

224

225   **Discussion**

226

227   This work provides a detailed retrospective analysis of the structural changes

228   seen in a large cohort of children with CHM. Until now, findings in this age group

229   have been scarce, and the few reported cases have been lost within a larger

230   volume of adult data. Consequently the earliest features of disease have been

231   poorly described.

232

233   Unlike most paediatric retinal dystrophies, which are discovered as a result of

234   reduced central acuity, CHM is most commonly identified as a result of

235   nyctalopia, and to a lesser degree loss of peripheral visual field. The youngest

236   patient to experience symptoms in this series was five years old, and so it is

237   likely that signs of retinopathy are present, yet undiscovered, at an early age.

238   With one exception, Patient 19, high refractive error was not a significant feature

239   of disease in keeping with other reports.[5] The low refractive error associated

240   with CHM also contrasts with the high myopia of X-linked retinitis pigmentosa

241   (XLRP), a potential phenocopy early in the disease course.

242

243   Maintenance of normal visual acuity is also in keeping with the absence of

244   significant macular oedema (MO), a feature reported to occur in up to 62.5% of

245   adult patients.[6] Early on in the disease course, a small increase in central retinal

246   thickness was noted in all patients with good central vision, perhaps indicating

247   subclinical microcystic oedema which was not easily visualised on OCT B scans.

248   Whilst the vast majority of eyes maintain baseline acuity, seven eyes recorded a

249   small deterioration in vision over the follow up period. The subfoveal retinal

250   thickness decreased in these eyes, acting perhaps as a surrogate marker of early

251   photoreceptor death. Over the same time period, almost all eyes showed a

252   reduction in subfoveal choroidal thickness. Despite the recognition of choroidal

253   atrophy in the first description of CHM, objective changes in choroidal thickness

254   have not previously been reported. Here we record a measurable reduction in

255   subfoveal choroidal thickness, detected at a time when central retinal function is

256   otherwise unaffected, and outside the zone of visible degeneration. This

257 discovery offers great clinical utility, as SD-OCT measurements of both retinal

258 and choroidal thickness, which have a low test-retest variability and can be

259 reliably obtained in virtually all subjects, will be useful both for monitoring

260 disease progression as well as response to novel therapies, independently of

261 visual acuity data.

262

263 Colour fundus photography was useful in identifying different stages of retinal

264 degeneration. Fourier et al. have previously used the same method to classify the

265 fundus changes present in female carriers of *CHM* mutations – mild RPE changes,

266 patchy RPE degeneration or confluent chorioretinal atrophy.[7] Identical

267 observations are reported here, but now in a paediatric cohort. Widespread

268 pigment clumping at the level of the RPE was identified as the earliest sign of

269 disease. This pigmentary response is very different to that observed in typical

270 retinitis pigmentosa, where RPE cells migrate into the neurosensory retina as a

271 consequence of photoreceptor cell death, usually resulting in a branched

272 network of "spicules". The pigment responsible for the observed changes has

273 two potential sources - melanosomes within the RPE, and melanocytes, thought

274 to be resident within the stroma of the choroid, both of which show significant

275 degeneration but for unknown reasons.[1] What *is* known is that REP-1

276 dysfunction, consequent upon *CHM* mutation, results in reduced Rab

277 prenylation.[8] Each Rab is uniquely sensitive to this process, based on its intrinsic

278 affinity for REP-1. Rab27a has a particularly low affinity when compared to other

279 Rabs, and as a result in a competitive environment, undergoes little prenylation.[8]

280 Rab27a dysfunction causes Griscelli syndrome (OMIM 607624), a disorder

281 characterized by hypomelanosis and immunological abnormalities. Rab27a is

282 now recognized not only as an important regulator of melanin transport in

283 melanosome, but also in polarized trafficking in (non-secretory) epithelial cells.[8]

284 It is therefore plausible that the observed retinal pigment clumping represents a

285 visible manifestation of local Rab27a-associated melanosome transport

286 dysfunction, and that other vesicle trafficking problems co-exist. Ultimately these

287 result in RPE disease and death. Unlike choroidal melanocytes, the RPE

288 melanosomes are fully mature at birth, and are incapable of renewal, perhaps

289 explaining why the RPE is so sensitive to REP-1 dysfunction.[9]

290

291 Following widespread pigmentary changes, well-defined regions of atrophy

292 develop, most commonly in the post-equatorial region, just outside the vascular

293 arcades. These changes advance centripetally whilst the far periphery seems to

294 be relatively spared. It is possible that this stereotypical feature of disease may

295 either relate to the underlying arrangement of lobular choroidal anatomy,

296 regional differences in RPE metabolism or indeed both, and explain why these

297 changes are not so readily seen in the anterior retina. A similar pattern of retinal

298 degeneration occurs in gyrate atrophy (OMIM 258870) and dominant mutation

299 of RPE65, but may also be observed in late-onset retinal degeneration (L-ORD,

300 OMIM 605670), all conditions that are thought to affect the RPE.[10]

301

302 Peri-papillary disease has been poorly described to date. In this series all

303 patients, even the youngest showed significant para- and peri-papillary atrophy.

304 Whilst objective analysis of the retinal nerve fibre layer in this region has been

305 performed, detailed assessment of the surrounding outer retina changes has not

306 been reported.[11-13] It is unclear why patients with CHM have early peri-papillary

307   involvement, whilst in retinal disease associated with biallelic *ABCA4* mutations

308   this retinal region is spared. One possibility is that choroidal blood flow may

309   influence the rate of progression, as degeneration in CHM appears to

310   preferentially occur in loci where the choroid is at its thinnest.

311

312   In addition to causing a progressive retinopathy, mutation of *CHM* could

313   theoretically also result in anatomical changes present at birth or shortly

314   thereafter. In keeping with this hypothesis, persistence of the inner retinal layers

315   was identified in approximately half of the cases (15/27), a similar finding to

316   that seen in patients with another disorder of hypomelanosis – albinism, where

317   variable degrees of foveal hypoplasia are observed.[14] In some cases however,

318   very dense scans through fixation were not obtained, so it remains possible that

319   a normal foveola exists but was just not captured. Usually however, the foveal pit

320   is large enough to be identifiable on at least two normal density macula line

321   scans, as such we feel that its absence is not due to technical factors. Again, in

322   keeping with incomplete foveal maturation, changes in central foveal

323   autofluorescence were also noted, perhaps indicating subtle alterations in the

324   amount of luteal pigment within Henle layer, a finding otherwise unexpected in

325   the earliest stages of many other retinal dystrophies. Lastly, macular hole

326   formation is an extremely uncommon complication of inherited retinal disease,

327   with only scattered single cases identified.[15] Unusually, a recent report describes

328   the prevalence of macular hole formation in patients with CHM at 10%, again

329   hinting at a possible underlying developmental macular anomaly.[16] Alternatively

330   this may either relate to a high prevalence of pre-retinal glial cell proliferation in

331   advanced disease resulting in mechanical traction from epiretinal membrane

332   tissue or the consequence of chronic cystic change.

333

334   Another feature associated with chorioretinal atrophy is ORT.[17] In our study ORT

335   was notably absent from regions of established atrophy, and only found adjacent

336   to healthy tissue, suggesting that the remaining (overhanging) photoreceptors

337   may organise themselves around residual islands of RPE cells. Other signs of

338   advanced atrophy, such as "ghost drusen" (highly reflective pyramidal

339   structures), a common feature of advanced L-ORD (unpublished observation),

340   are absent. Similarly, although late-stage retinal disease may also be complicated

341   by choroidal neovascularization (CNVM), this is thought to be an uncommon

342   feature of end-stage CHM. Cases of presumed CNVM, similar to that observed in

343   patient 10 do exist, and have been reported by others.[18] The true prevalence of

344   CNVM will be hard to determine however, as generally only symptomatic

345   patients are identified.

346

347   This study provides a detailed description of the clinical, imaging and genetic

348   findings present in a large cohort of paediatric patients with CHM. We propose

349   that the observed widespread pigmentary changes are a visible consequence of

350   Rab27a dysfunction, and highlight novel anatomical changes present both in the

351   peri-papillary retina and inner retina at the fovea. In addition, we have presented

352   SD-OCT data demonstrating a reduction in subfoveal choroidal thickness with

353   disease progression, and a simultaneous increase in foveal retinal thickness, both

354   of which occur whilst visual acuity is maintained. Deterioration in visual acuity is

355   uncommon in CHM in childhood but when it does occur it is associated with a

356   reduction in retinal thickness. The anatomical changes described herein were

357 evident even in the youngest patients, and hence must occur early in the disease

358 course. We envisage that these objective imaging parameters will become useful

359 tools for monitoring change, both in prospective natural history studies of CHM

360 and in response to future treatments.

361 **<u>RFERENCES</u>**

362

363 1.   Coussa RG, Traboulsi EI. Choroideremia: A review of general findings and

364 pathogenesis. Ophthalmic Genetics 2012;33(2):57-65.

365 2.   Cremers F, 6Uniuersitéitszugenklinik EKU. Molecular Basis of

366 Choroideremia (CHM): Mutations involving the Rab Escort Proteinal (REP-1)

367 Gene. Human mutation 1997;9:110-7.

368 3.   Leung KF, Baron R, Seabra MC. Thematic review series: lipid

369 posttranslational modifications. geranylgeranylation of Rab GTPases. J Lipid Res

370 2006;47(3):467-75.

371 4.   Pereira-Leal JB, Hume AN, Seabra MC. Prenylation of Rab GTPases:

372 molecular mechanisms and involvement in genetic disease. FEBS letters

373 2001;498(2):197-200.

374 5.   Seitz IP, Zhour A, Kohl S, et al. Multimodal assessment of choroideremia

375 patients defines pre-treatment characteristics. Graefe's Archive for Clinical and

376 Experimental Ophthalmology 2015:1-8.

377 6.   Genead MA, Fishman GA. Cystic macular oedema on spectral-domain

378 optical coherence tomography in choroideremia patients without cystic changes

379 on fundus examination. Eye 2011;25(1):84-90.

380   7.   Forius H, Hyvainen L, Nieminen H, Flower R. FLuorescein and

381   Indocyanine green Fluorescence angiography in study of affected males and in

382   female carriers with Choroidermia. Acta ophthalmologica 1977;55(3):459-70.

383   8.   Köhnke M, Delon C, Hastie ML, et al. Rab GTPase prenylation hierarchy

384   and its potential role in choroideremia disease. PloS one 2013;8(12):e81758.

385   9.   Nag TC. Ultrastructural changes in the melanocytes of aging human

386   choroid. Micron 2015;79:16-23.

387   10.   Bowne SJ, Humphries MM, Sullivan LS, et al. A dominant mutation in

388   RPE65 identified by whole-exome sequencing causes retinitis pigmentosa with

389   choroidal involvement. Eur J Hum Genet 2011;19(10):1074-81.

390   11.   Genead MA, McAnany JJ, Fishman GA. Retinal nerve fiber thickness

391   measurements in choroideremia patients with spectral-domain optical

392   coherence tomography. Ophthalmic genetics 2011;32(2):101-6.

393   12.   Jiang R, Wang YX, Wei WB, et al. Peripapillary Choroidal Thickness in

394   Adult Chinese: The Beijing Eye StudyPeripapillary Choroidal Thickness.

395   Investigative ophthalmology & visual science 2015;56(6):4045-52.

396   13.   Read SA, Alonso-Caneiro D, Vincent SJ, Collins MJ. Peripapillary choroidal

397   thickness in childhood. Experimental eye research 2015;135:164-73.

398   14.   Lee H, Purohit R, Sheth V, et al. Retinal development in albinism: a

399   prospective study using optical coherence tomography in infants and young

400   children. The Lancet 2015;385:S14.

401   15.   Sodi A, Bini A, Passerini I, et al. Occurrence of full-thickness macular hole

402   complicating Stargardt disease with ABCR mutation. Eur J Ophthalmol

403   2006;16(2):335-8.

404   16.   Zinkernagel MS, Groppe M, MacLaren RE. Macular hole surgery in patients

405   with end-stage choroideremia. Ophthalmology 2013;120(8):1592-6.

406   17.   Iriyama A, Aihara Y, Yanagi Y. Outer retinal tubulation in inherited retinal

407   degenerative disease. Retina 2013;33(7):1462-5.

408   18.   Palejwala NV, Lauer AK and Weleber RG. Choroideremia associated with

409   choroidal neovascularization treated with intravitreal bevacizumab. Clinical

410   Ophthalmology 2014 8:1675-1679.

411

412

413   **LEGENDS**

414   Figure 1: Colour fundus photography in patients with choroideraemia. (a) Early,

415   fine, granular pigmentary changes in the central macula and around the vascular

416   arcades, (b) larger pigment plaques in the temporal periphery. (c) Four years

417   later the regions of pigmentary change have now evolved to atrophy, also

418   involving the peripapillary retina (patient 4). Images (d, e) and (f, g) taken from

419   patient 5 two years apart, highlighting progressive PPA. (h, i) Optos

420   pseudocolour images from patient 7 highlighting well defined scalloped atrophy

421   and pigment plaques with less well-defined anterior changes.

422

423   Figure 2: Fundus autofluorescence images demonstrating the progression in

424   peripapillary atrophy in patient 2 (a, b). Three distinct zones of autofluorescence

425   are visible in patient 6 – complete absence, speckled and normal (c, d).

426

427   Figure 3: Spectral domain optical coherence tomography in patients with

428   choroideraemia. Approximately half of all eyes demonstrated persistence of the

429   inner retinal layers (a, b). In regions immediately adjacent to atrophic retina, loss

430   of retinal structure was associated with the presence of cystic spaces in either

431   the outer or inner nuclear layers (c). Outer retinal tubulations were observed

432   only in regions retaining small islands of retinal pigment epithelium, but never in

433   areas of frank atrophy (d). Imaging the left eye of Patient 10 shows the presence

434   of highly reflective subretinal material, suggestive of prior choroidal

435   neovascularization (e).

436

Table

Table 1. Patient demographics

	Age	Refraction RE	Refraction LE	Mutation	Follow up (years)	ΔVA (RE/LE) [decimal Snellen/year]	ΔRetinal thickness (RE/LE) [μm/month]	ΔChoroidal thickness (RE/LE) [μm/month]	ΔBAF area (RE/LE) [mm²/month]
1	13	n/a	n/a	Tyr42Ter	12.9	0, 0	6.3, -1.5	-9.5, -4.5	0.36, 0.25
2	10	n/a	n/a	no testing	11.0	0, 0			-
3	16	+0.75/-0.25x90	-0.50/-0.25x55	p.Lys415AsnfsX4	9..2	0, 0	2.3, 1.3	-13.6, -11	-
4	5	n/a	n/a	c.G2931insA, p.Glu311fs	9..6	0, 0	-	-	-
5	12	-1.50/-0.75x70	-0.75/-1.25x85	deletion exons 1-11	9..2	0, 0	3.3, 6.6	-1.3, -0.3	3.15, 3.5
6	10	-2.00/-0.25x45	-1.75/-0.25x120	c.525_526delAG	13.5	0, 0	-0.6, -7.4	0, -3.6	0.2, 0.6
7	4	+2.50DS	+2.50DS	no testing	9.4	0, 0	11, 8.6	-23.3, -10	2.4, 5.35
8	9	+2.50/-0.50x90	+1.75/-0.50x70	whole gene deletion	10.1	+0.33, +0.33	6.5, 6.5	-10, 0	-
9	3	+3.00/-0.50x180	+3.00DS	no testing	8.7	0, 0	9.5, 17.5	-36.5, -40	-
10	3	+2.00/-0.50x180	+2.00/-0.50x180	no testing	12.0	0, 0	-	-	-
11	8	+3.25/-0.50x90	+3.00/-0.25x90	negative screen	4.2	0, +0.33	-	-	-
12	9	+2.50/0.25x180	+2.50DS	no testing	1.0		9.5, 17.5	-	-
13	7	+2.75/-0.25x180	+2.00/-0.50x180	no testing	6.7	+0.58, +0.58	-	-17.6, -21.5	-
14	12	+2.75/-0.50x50	+2.75/-0.50x140	c.703-1_727delins TTAGA	0.6	0, 0	-	-	-
15	10	-	-	negative screen	6.6	0, 0	0.8, 1.5	-0.5, -1.3	-
16	15	-0.75/-1.75x10	-0.25/-2.00x170	c.831delC	3.6	0, 0	3, 3.5	-4, -4	-
17	15	-1.75/+1.25x95	-1.50/+1.50x80	no testing	1.0	0, 0	-	-	-
18	6	+2.00/-0.25x20	+2.75/-1.25x160	no testing	Single visit	-	-	-	-
19	12	+7.5/+1.75x5	+8.0/-1.50x180	p.Asn360ThrfsX49	3.9	0.14, 0.16	-	-	-
20 – twin 1	7	+2.50/-0.50x20	+2.50/-0.50x160		5.6	0, 0	11.6, 8	0.3, 4.3	-
21 – twin 2	7	+2.25DS	+2.00DS	negative screen in mother	5.6	0, 0	2.6, 2.3	-3.3, -10.6	-
22	10	+4.00/-1.50x180	+4.00/-1.50x10	no testing	4.0	0, 0	3.3, 2.3	-25.6, -15.6	-
23	14	-	-	p.Arg253Ter not present in mother	3.7	-0.33, -0.33	-	-	-
24	7	+4.00/-0.25x180	+4.00/0.50x180	no testing	3.7	-0.1, -0.1	-18, -24	-61, -35	-
25	15	-0.75DCx20	0.50DCx160	c.282delT	1.0	0.50,0.24	-	-	-
26	6	+2.25DS	+2.50DS	c.675dupG	1.25	0, 0	13, -6	-3, -4	-
27	10	-	-	del intron 1-7	1.2	-0.1, -0.1	-6, -4	-44, -1	-
28	7	+2.0DS	+1.75DS	pArg270Ter	1.25	0, -0.1	-16, -6	-17, -17	-
29	6	+1.25/-1.25x165	0.75/-1.50x7.5	c.1349+1delG	1.5	0, 0	-	-	-

RE = right eye, LE = left eye, VA = visual acuity, - = not performed

Table

Table 1. Patient demographics

	Age	Refraction RE	Refraction LE	Mutation	Follow up (years)	ΔVA (RE/LE) [decimal Snellen/ year]	ΔRetinal thickness (RE/LE) [μm/month]	ΔChoroidal thickness (RE/LE) [μm/ month]	ΔBAF area (RE/LE) [mm²/ month]
1	13	n/a	n/a	Tyr42Ter	13	0, 0	6.3, -1.5	-9.5, -4.5	0.36, 0.25
2	10	n/a	n/a	no testing	11	0, 0			-
3	16	+0.75/-0.25x90	-0.50/-0.25x55	p.Lys415AsnfsX4	9	0, 0	2.3, 1.3	-13.6, -11	-
4	5	n/a	n/a	c.G2931insA, p.Glu311fs	10	0, 0	-	-	-
5	12	-1.50/-0.75x70	-0.75/-1.25x85	deletion exons 1-11	9	0, 0	3.3, 6.6	-1.3, -0.3	3.15, 3.5
6	10	-2.00/-0.25x45	-1.75/-0.25x120	c.525_526delAG	13	0, 0	-0.6, -7.4	0, -3.6	0.2, 0.6
7	4	+2.50DS	+2.50DS	no testing	9	0, 0	11, 8.6	-23.3, -10	2.4, 5.35
8	9	+2.50/-0.50x90	+1.75/-0.50x70	whole gene deletion	10	+0.33, +0.33	6.5, 6.5	-10, 0	-
9	3	+3.00/-0.50x180	+3.00DS	no testing	8	0, 0	9.5, 17.5	-36.5, -40	-
10	3	+2.00/-0.50x180	+2.00/-0.50x180	no testing	12	0, 0	-	-	-
11	8	+3.25/-0.50x90	+3.00/-0.25x90	negative screen	4	0, +0.33	-	-	-
12	9	+2.50/0.25x180	+2.50DS	no testing	1		9.5, 17.5	-	-
13	7	+2.75/-0.25x180	+2.00/-0.50x180	no testing	7	+0.58, +0.58	-	-17.6, -21.5	-
14	12	+2.75/-0.50x50	+2.75/-0.50x140	c.703-1_727delins TTAGA	0.6	0, 0	-	-	-
15	10	-	-	negative screen	7	0, 0	0.8, 1.5	-0.5, -1.3	-
16	15	-0.75/-1.75x10	-0.25/-2.00x170	c.831delC	3	0, 0	3, 3.5	-4, -4	-
17	15	-1.75/+1.25x95	-1.50/+1.50x80	no testing	1	0, 0	-	-	-
18	6	+2.00/-0.25x20	+2.75/-1.25x160	no testing	0	-	-	-	-
19	12	+7.5/+1.75x5	+8.0/-1.50x180	p.Asn360ThrfsX49	4	0.14, 0.16	-	-	-
20 – twin 1	7	+2.50/-0.50x20	+2.50/-0.50x160		6	0, 0	11.6, 8	0.3, 4.3	-
21 – twin 2	7	+2.25DS	+2.00DS	negative screen in mother	6	0, 0	2.6, 2.3	-3.3, -10.6	-
22	10	+4.00/-1.50x180	+4.00/-1.50x10	no testing	4	0, 0	3.3, 2.3	-25.6, -15.6	-
23	14	-	-	p.Arg253Ter not present in mother	3	-0.33, -0.33	-	-	-
24	7	+4.00/-0.25x180	+4.00/0.50x180	no testing	3	-0.1, -0.1	-18, -24	-61, -35	-
25	15	-0.75DCx20	0.50DCx160	c.282delT	0	0.50,0.24	-	-	-
26	6	+2.25DS	+2.50DS	c.675dupG	1	0, 0	13, -6	-3, -4	-
27	10	-	-	del intron 1-7	1	-0.1, -0.1	-6, -4	-44, -1	-
28	7	+2.0DS	+1.75DS	pArg270Ter	1	0, -0.1	-16, -6	-17, -17	-
29	6	+1.25/-1.25x165	0.75/-1.50x7.5	c.1349+1delG	1	0, 0	-	-	-

RE = right eye, LE = left eye, VA = visual acuity, - = not performed

Figure 1
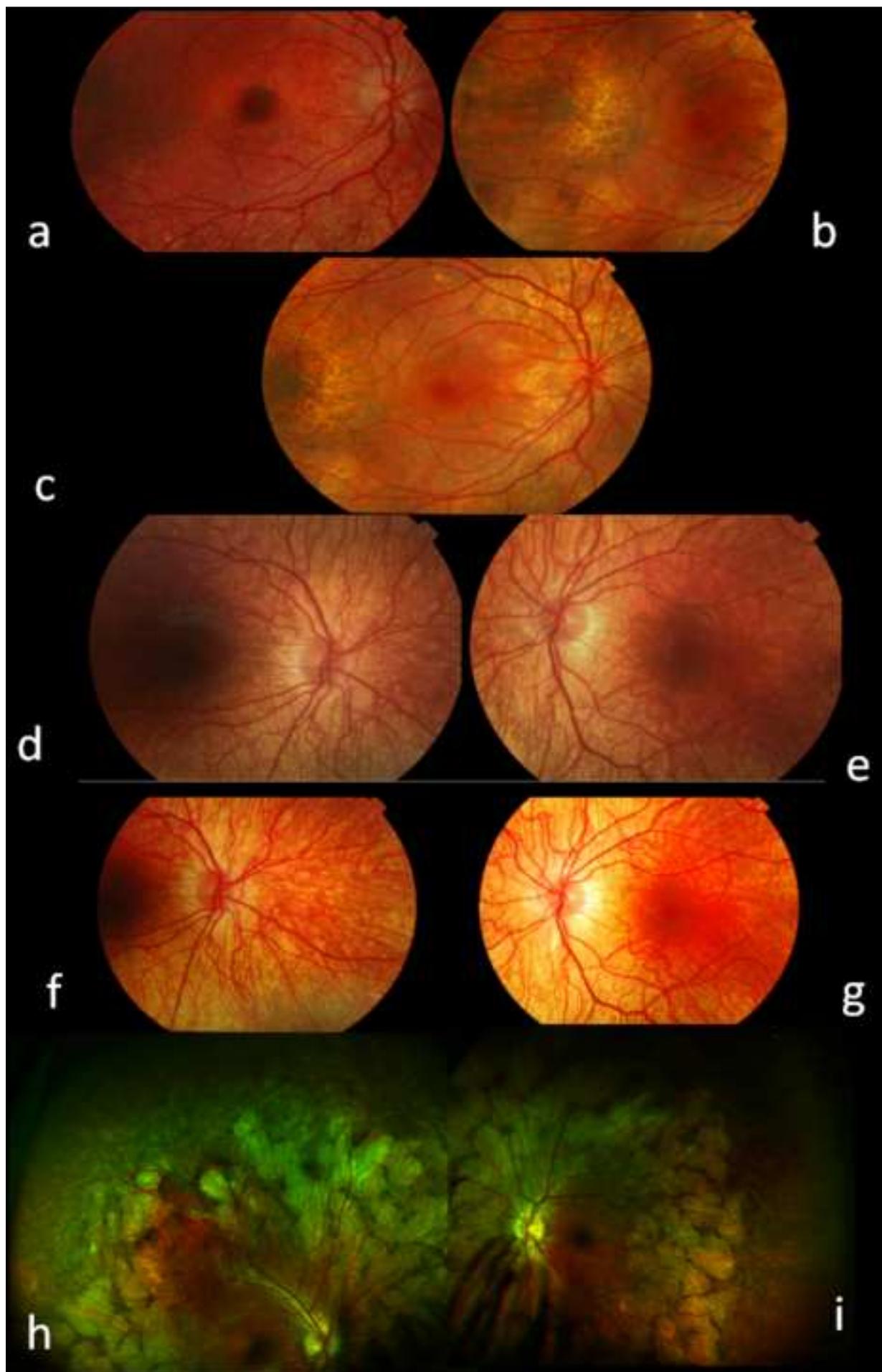**Click here to download high resolution image**

Figure 2
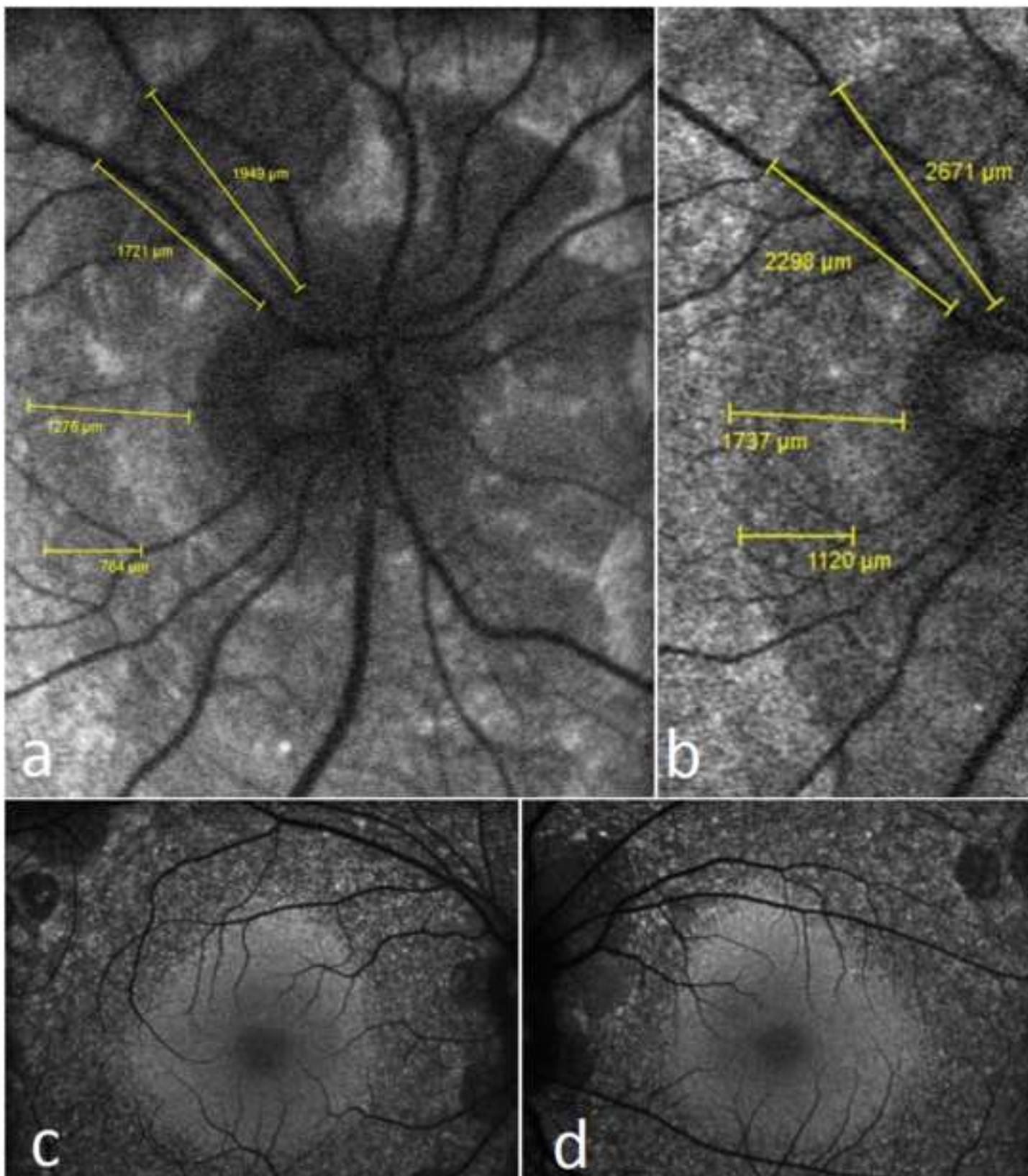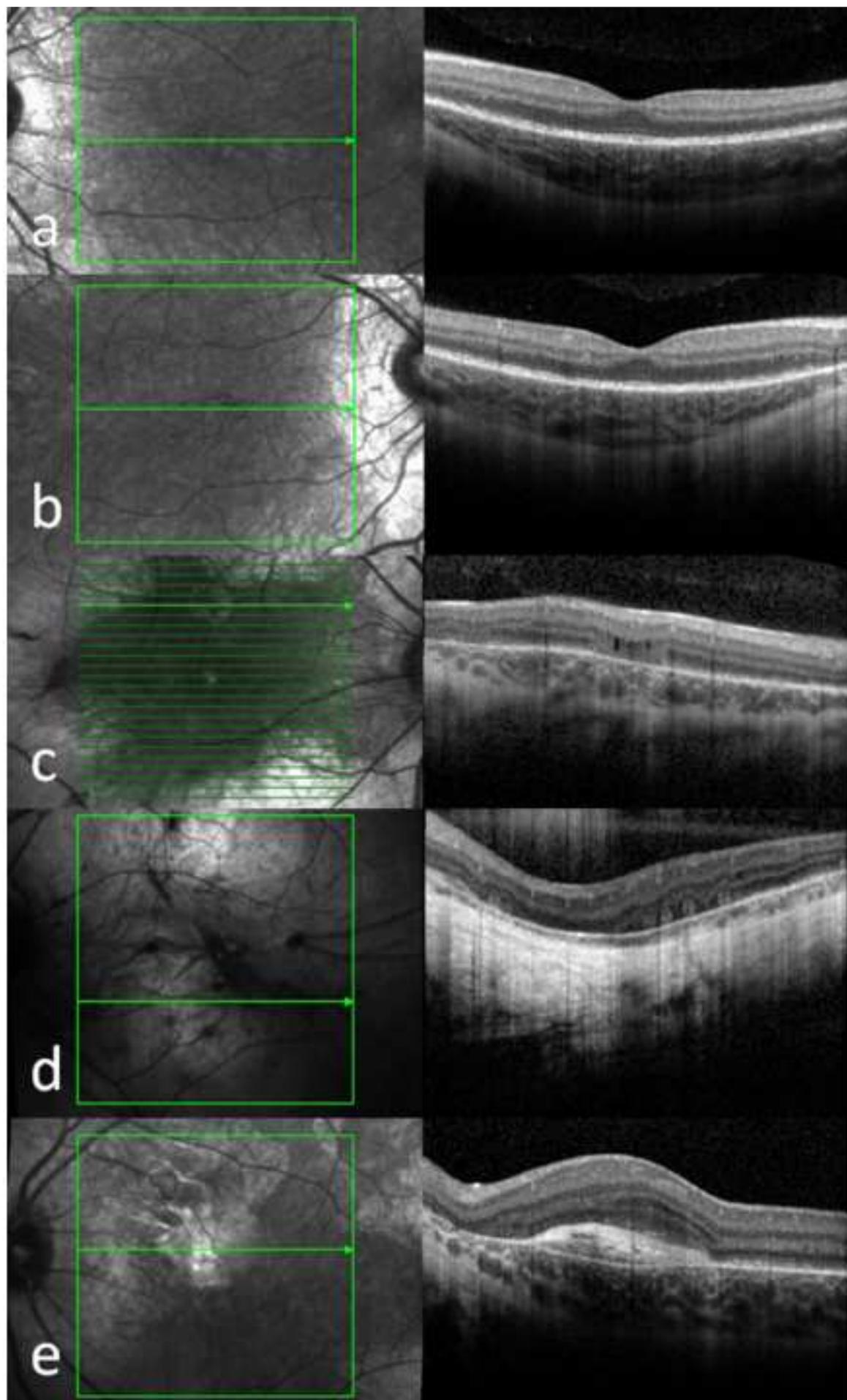**Click here to download high resolution image**

Figure 3
[Click here to download high resolution image](#)

*Conflict of Interest Form (ICMJE COI)

[Click here to download Conflict of Interest Form (ICMJE COI): coi_disclosure_moore.pdf](coi_disclosure_moore.pdf)

*Conflict of Interest Form (ICMJE COI)
Click here to download Conflict of Interest Form (ICMJE COI): coi_disclosure_islam.pdf

*Conflict of Interest Form (ICMJE COI)

*Conflict of Interest Form (ICMJE COI)
Click here to download Conflict of Interest Form (ICMJE COI): coi_disclosure_khan.pdf

*Author Contributorship Form